

DELAMINATION OF MULTILAYERED BEAMS WITH
NON-LINEAR VISCOELASTIC BEHAVIOUR UNDER STRAINS
OF STEP-LIKE VARYING VELOCITY

V. RIZOV^{1*}, H. ALTENBACH²

¹*Department of Technical Mechanics,
University of Architecture, Civil Engineering and Geodesy,
1 Chr. Smirnensky blvd. 1046 - Sofia, Bulgaria*

²*Lehrstuhl für Technische Mechanik, Fakultät für Maschinenbau,
Otto-von-Guericke-Universität Magdeburg,
Universitätsplatz 2, 39106 Magdeburg, Deutschland*

[Received: 17 January 2022. Accepted: 17 November 2022]

doi: <https://doi.org/10.55787/jtams.23.53.2.099>

ABSTRACT: The present paper deals with delamination analysis of a multilayered inhomogeneous beam structure that exhibits non-linear viscoelastic behaviour under strains whose velocity varies step-like with time. There are two delaminations in the beam. The left-hand delamination crack arm is subjected to bending so as the velocity of angle of rotation of this crack arm varies step-like with time. A non-linear viscoelastic model with a spring and two dashpots treats the beam mechanical behaviour. Solutions of the strain energy release rate are derived for both delaminations. A parametric investigation of delamination in the beam is carried-out by using the solutions.

KEY WORDS: inhomogeneous beam, multilayered material, delamination, material non-linearity, viscoelastic behaviour.

1 INTRODUCTION

The use of modern structural materials with superior properties in various engineering applications has been significantly increased in recent years. These materials include, for instance, the group of inhomogeneous materials whose properties vary continuously within the structural component. The properties of the continuously inhomogeneous materials are smooth functions of coordinates. Functionally graded materials belong to this group [1–3]. In fact, the functionally graded materials are class of continuously inhomogeneous composites that are composed usually of two material phases. Graded distribution of material properties is formed by gradually

*Corresponding author e-mail: v_rizov_fhe@uacg.bg

changing the ratio of material phases in the volume of a functionally graded structural member during manufacturing [4–6]. One of the distinct advantages of the conception of functionally graded materials is that it permits controlled tailoring of the spatial variation of material properties. Due to the excellent functional characteristics, functionally graded materials have attracted worldwide attention. They have been widely used in critical structural applications in aeronautics, nuclear reactors, and other mechanical applications. Many investigations and theoretical research of mechanics of various continuously inhomogeneous (functionally graded) structural members have been carried-out in the recent decades [7–9].

Multilayered inhomogeneous structural materials are built-up of adhesively bonded layers of dissimilar materials. The fact that the multilayered materials have high strength-to-weight and stiffness-to-weight ratios is the most important argument for using them in lightweight constructions and in other engineering applications where the weight is a concern [10–12]. Separation of layers known as delamination is one of the most important reasons for limited application of multilayered materials in critical load-bearing structures.

The advance in the up-to-date theory of multilayered engineering structures is closely related with analysis of varied problems in the area of delamination and rheology of structural materials. The assessment of delamination processes in materials and load-bearing structures, which exhibit time-dependent mechanical behaviour under different loading conditions and external influences, is very important in the context of ensuring of technical safety and reliability of multilayered structures. Lapses in delamination analyses may have catastrophic consequences for technical constructions and facilities including entire collapse.

The present paper aims to develop a delamination analysis of a non-linear viscoelastic multilayered inhomogeneous beam structure with two delaminations subjected to strains whose velocity varies step-like with time. This analysis is needed since in various engineering applications multilayered inhomogeneous beams under changeable loadings exhibit non-linear viscoelastic behaviour. It should be noted that previous studies deal mainly with delamination analyses of linear viscoelastic inhomogeneous beams under constant or smoothly changing loadings [13, 14]. Thus, the present paper develops further the analyses presented in [13, 14] by considering non-linear viscoelastic behaviour and a more complex external loading. Solutions of the strain energy release rate are found here for both delaminations with considering of the step-like variation of the strain velocity with time.

2 ANALYSIS OF THE STRAIN ENERGY RELEASE RATE WITH CONSIDERING OF NON-LINEAR VISCOELASTIC BEHAVIOUR UNDER STEP-LIKE VARYING STRAIN VELOCITY

The multilayered non-linear viscoelastic beam displayed in Fig. 1 is made of m layers of different widths and material properties. The layers are continuously inhomogeneous along their widths. The beam is clamped in section, R . The width, height and length of the beam are denoted by b , h and l , respectively. Two delamination cracks are located in the beam (Fig. 1). The lengths of the left-hand and right-hand delamination cracks are denoted by a_1 and a_2 , respectively, where $a_1 < a_2$. The widths of the left-hand, middle and right-hand delamination crack arms are b_1 , b_2 and b_3 , respectively. The left hand crack arm is loaded in pure bending so as the velocity, v_ϕ , of the angle of rotation, ϕ , of the free end of this crack arm varies step-like with time, t , as displayed in Fig. 2. The velocity of ϕ at $t_{i-1} \leq t \leq t_i$ is $v_{\phi i}$ (Fig. 2). The middle and the right-hand delamination crack arms are free of stresses.

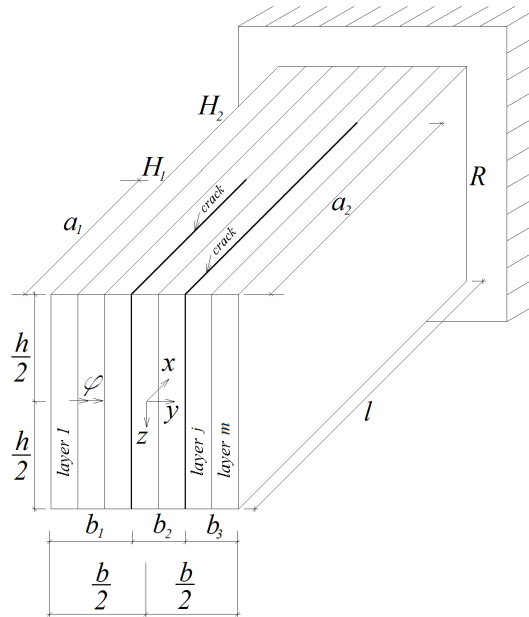


Fig. 1: Multilayered non-linear viscoelastic beam with two delaminations.

The variation of ϕ with time is displayed in Fig. 3. At $t_{i-1} \leq t \leq t_i$ the angle, ϕ , is expressed as (Fig. 3)

$$(1) \quad \phi = \phi_{pi-1} + v_{\phi i} (t - t_{i-1}),$$

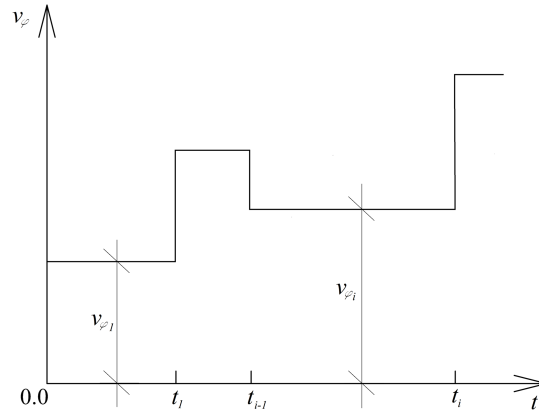


Fig. 2: Step-like variation of the velocity of the angle of rotation of the left-hand crack arm free end with time.

where

$$(2) \quad i = 1, 2, \dots s.$$

In formulae (1) and (2), ϕ_{pi-1} is the angle of rotation at $t = t_{i-1}$, s is the number of steps of v_ϕ . Figure 3 indicates that $\phi_{p0} = 0$.

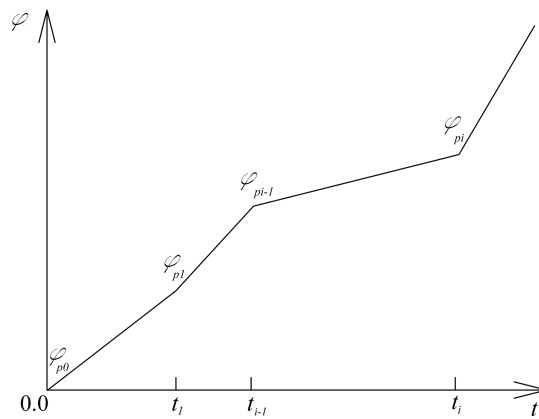


Fig. 3: Variation of the angle of rotation with time.

The non-linear viscoelastic model used to describe the mechanical behaviour of the j -th layer of the beam is displayed in Fig. 4. The model has a linear spring with modulus of elasticity, E_j , a linear dashpot with coefficient of viscosity, η_j , and a non-linear dashpot, (nld_j) , assembled as displayed in Fig. 4. The following power law

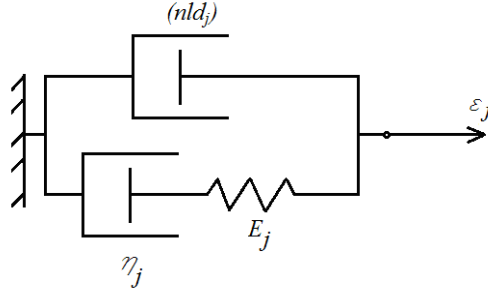


Fig. 4: Non-linear viscoelastic model.

describes the behaviour of the non-linear dashpot:

$$(3) \quad \sigma_{nldj} = \eta_{nldj} (\dot{\varepsilon}_j)^{\frac{1}{n_j}},$$

where

$$(4) \quad j = 1, 2, \dots, m.$$

In formula (3), σ_{nldj} is the stress in the dashpot, $\dot{\varepsilon}_j$ is the first derivative of the strain with respect to time, η_{nldj} and n_j are material properties.

The model in Fig. 4 is subjected to strain, ε_j , whose velocity, $v_{\varepsilon j}$, varies step-like with time. At $t_{i-1} \leq t \leq t_i$ the velocity of the strain is $v_{\varepsilon j i}$. The variation of the strain with time at $t_{i-1} \leq t \leq t_i$ is found as

$$(5) \quad \varepsilon_j = \varepsilon_{pji-1} + v_{\varepsilon j i} (t - t_{i-1}),$$

where

$$(6) \quad i = 1, 2, \dots, s.$$

In formula (5), ε_{pji-1} is the strain at $t = t_{i-1}$. It should be noted that $\varepsilon_{pj0} = 0$ at $t = 0$.

The constitutive law of the model in Fig. 4 is derived by using the following relationships:

$$(7) \quad \sigma_{Ej} = \sigma_{\eta j},$$

$$(8) \quad \sigma_{Ej} = E_j \varepsilon_{Ej},$$

$$(9) \quad \sigma_{\eta j} = \eta_j \dot{\varepsilon}_{\eta j},$$

$$(10) \quad \varepsilon_{Ej} + \varepsilon_{\eta j} = \varepsilon_j,$$

where σ_{Ej} and $\sigma_{\eta j}$ are, respectively, the stresses in the linear spring and linear dashpot, ε_{Ej} and $\varepsilon_{\eta j}$ are the strains in the linear spring and linear dashpot, respectively. By combining of (5)–(10), one obtains

$$(11) \quad \dot{\varepsilon}_{\eta j} + \beta_j \varepsilon_{\eta j} = \delta_j + \rho_j t,$$

where

$$(12) \quad \beta_j = \frac{E_j}{\eta_j},$$

$$(13) \quad \delta_j = \frac{E_j \varepsilon_{pj i-1}}{\eta_j} - \frac{E_j v_{\varepsilon j i} t_{i-1}}{\eta_j},$$

$$(14) \quad \rho_j = \frac{E_j v_{\varepsilon j i}}{\eta_j}.$$

Since (11) is inhomogeneous differential equation, its solution is written as

$$(15) \quad \varepsilon_{\eta j} = C_1 e^{-\beta_j t} + \bar{\varepsilon}_{\eta j},$$

where C_1 is an integration constant, $\bar{\varepsilon}_{\eta j}$ is a particular solution which is determined as

$$(16) \quad \bar{\varepsilon}_{\eta j} = B_j + D_j t,$$

where B_j and D_j are constants. By substituting of $\bar{\varepsilon}_{\eta j}$ and $\dot{\bar{\varepsilon}}_{\eta j}$ in (11), one derives

$$(17) \quad B_j = \frac{1}{\beta_j} \left(\delta_j - \frac{\rho_j}{\beta_j} \right),$$

$$(18) \quad D_j = \frac{\rho_j}{\beta_j}.$$

The initial condition used to determine the integration constant in (15) is written as

$$(19) \quad \varepsilon_{\eta j}(t_{i-1}) = \varepsilon_{pj i-1}.$$

Combining of (15) and (19), one obtains

$$(20) \quad C_1 = \frac{1}{e^{-\beta_j t_{i-1}}} (\varepsilon_{pj i-1} - B_j - D_j t_{i-1}).$$

The substitution of (16) and (20) in (15) results in

$$(21) \quad \varepsilon_{\eta j}(t) = e^{\beta_j(t_{i-1}-t)} (\varepsilon_{pj i-1} - B_j - D_j t_{i-1}) + B_j + D_j t.$$

By using (9) and (21), the stress in the linear dashpot is determined as

$$(22) \quad \sigma_{\eta j} = \eta_j \left[e^{\beta_j(t_{i-1}-t)} \beta_j (-\varepsilon_{pji-1} + B_j + D_j t_{i-1}) + D_j \right].$$

Combining of (3) and (5), the stress in the non-linear dashpot is derived as

$$(23) \quad \sigma_{nldj} = \eta_{nldj} v_{\varepsilon_{ji}}^{\frac{1}{n_j}}.$$

The stress in the non-linear viscoelastic model is found as (Fig. 4)

$$(24) \quad \sigma_j = \sigma_{\eta j} + \sigma_{nldj}.$$

The substitution of (22) and (23) in (24) yields

$$(25) \quad \sigma_j = \eta_j \left[e^{\beta_j(t_{i-1}-t)} \beta_j (-\varepsilon_{pji-1} + B_j + D_j t_{i-1}) + D_j \right] + \eta_{nldj} v_{\varepsilon_{ji}}^{\frac{1}{n_j}}.$$

By combining of (12), (13), (24), (17), (18) and (25), one derives

$$(26) \quad \sigma_j = \eta_j e^{\beta_j(t_{i-1}-t)} (\beta_j t_{i-1} - 1) \frac{\varepsilon_j - \varepsilon_{pji-1}}{t - t_{i-1}} + \eta_{nldj} \left(\frac{\varepsilon_j - \varepsilon_{pji-1}}{t - t_{i-1}} \right)^{\frac{1}{n_j}}.$$

Relationship (26) holds at $t_{i-1} \leq t \leq t_i$, where $i = 1, 2, \dots, s$.

The layers exhibit continuous material inhomogeneity along the width. Thus, the material properties, E_j , η_j and η_{nldj} , vary continuously in the direction of width. Their variation is described as

$$(27) \quad E_j = E_{0j} e^{\lambda_j \frac{y-y_j}{y_{j+1}-y_j}},$$

$$(28) \quad \eta_j = \eta_{0j} e^{\mu_j \frac{y-y_j}{y_{j+1}-y_j}},$$

$$(29) \quad \eta_{nldj} = \eta_{0nldj} e^{\omega_j \frac{y-y_j}{y_{j+1}-y_j}},$$

where

$$(30) \quad y_j \leq y \leq y_{j+1},$$

$$(31) \quad j = 1, 2, \dots, m.$$

In formulae (27) – (30), E_{0j} , η_{0j} and η_{0nldj} are, respectively, the values of E_j , η_j and η_{nldj} at the left-hand lateral surface of the j -the layer, λ_j , μ_j and ω_j are parameters which control the variation of E_j , η_j and η_{nldj} , respectively, y_j and y_{j+1}

are the coordinates of the left-hand and right-hand lateral surfaces of the layer, y is the horizontal centric axis the beam cross-section.

The strain energy release rate is derived by analysing the balance of the energy. First, the left-hand delamination is considered. The balance of the energy is written as

$$(32) \quad M\delta\phi = \frac{\partial U}{\partial a_1}\delta a_1 + G_1 h \delta a_1,$$

where U is the strain energy in the beam, G_1 is the strain energy release rate for the left-hand crack arm. Using (32), one obtains

$$(33) \quad G_1 = \frac{1}{h} \left(M \frac{\partial \phi}{\partial a_1} - \frac{\partial U}{\partial a_1} \right).$$

Since only the left-hand delamination crack arm is loaded (Fig. 1), the middle delamination crack arm in portion, $0 \leq x \leq a_1$, and the right-hand delamination crack arm, $0 \leq x \leq a_2$, are free of stresses (here, x is the longitudinal centroidal axis). Therefore, the strain energy in the beam is found as

$$(34) \quad U = U_L + U_Q + U_F,$$

where U_L , U_Q and U_F are the strain energies in portions, $0 \leq x \leq a_1$ and $a_1 \leq x \leq a_2$, of the left-hand crack arm, and in the un-cracked beam portion, $a_2 \leq x \leq l$, respectively.

The strain energy, U_L , is expressed as

$$(35) \quad U_L = a_1 \sum_{j=1}^{j=m_L} \int_{-\frac{h}{2}}^{\frac{h}{2}} \left(\int_{y_{1j}}^{y_{1j+1}} u_{0Lj} dy_1 \right) dz_1,$$

where m_L is the number of layers in portion, $0 \leq x \leq a_1$, of the left-hand crack arm, y_{1j} and y_{1j+1} are the coordinates of the left-hand and right-hand lateral surfaces of the j -th layer, u_{0Lj} is the strain energy density, y_1 and z_1 are the horizontal and vertical centric axes of the cross-section of this crack arm.

The strain energy density is written as:

$$(36) \quad u_{0Lj} = \int_0^{\varepsilon_j} \sigma_j d\varepsilon_j.$$

By substituting of (26) in (36), one obtains

$$(37) \quad u_{0Lj} = \frac{1}{2}\theta_i\varepsilon_j^2 - \theta_i\varepsilon_{pji-1}\varepsilon_j + \frac{\eta m d_j n_j}{(1+n_j)(t-t_{i-1})^{\frac{1}{n_j}}} \left[(\varepsilon_j - \varepsilon_{pji-1})^{\frac{1+n_j}{n_j}} - (-\varepsilon_{pji-1})^{\frac{1+n_j}{n_j}} \right],$$

where

$$(38) \quad \theta_j = \eta_j e^{\beta_j(t_{i-1}-t)} (\beta_j t_{i-1} - 1) \frac{1}{t - t_{i-1}}.$$

The distribution of strains is analyzed by applying the Bernoulli's hypothesis for plane sections since the length to height ratio of the beam structure under consideration is high. Thus, the distribution of ε_j along the height of the left-hand crack arm is written as

$$(39) \quad \varepsilon_j = \kappa_L z_1,$$

where

$$(40) \quad -\frac{h}{2} \leq z_1 \leq \frac{h}{2}.$$

In formula (39), κ_L is the curvature of the crack arm.

The curvature is determined by the following approach. First, the equation of equilibrium of the bending moments in cross-section, H_1 , of the left-hand crack arm is written as

$$(41) \quad \sum_{j=1}^{j=m_L} \int_{-\frac{h}{2}}^{\frac{h}{2}} \left(\int_{y_{1j}}^{y_{1j+1}} \sigma_j z_1 dy_1 \right) dz_1 = \sum_{j=1}^{j=m_Q} \int_{-\frac{h}{2}}^{\frac{h}{2}} \left(\int_{y_{2j}}^{y_{2j+1}} \sigma_{Qj} z_2 dy_2 \right) dz_2,$$

where σ_j is found by (26). The strain, ε_j , that is involved in (26) is obtained by (39). In equation (41), m_Q is the number of layers in portion, $a_1 \leq x \leq a_2$, of the left-hand crack arm, y_{2j} and y_{2j+1} are the coordinates of the left-hand and right-hand lateral surfaces of the layer, σ_{Qj} is the stress that is found by replacing of ε_j with ε_{Qj} in formula (26). Here, ε_{Qj} is obtained by replacing of κ_L with κ_Q in (39) where κ_Q is the curvature of the left-hand crack arm in portion, $a_1 \leq x \leq a_2$.

Another equation is composed by considering the equilibrium of the bending moments in cross-section, H_2 , of the left-hand crack arm and the un-cracked portion of

the beam

$$(42) \quad \sum_{j=1}^{j=m_Q} \int_{-\frac{h}{2}}^{\frac{h}{2}} \left(\int_{y_{2j}}^{y_{2j+1}} \sigma_{Qj} z_2 dy_2 \right) dz_2 = \sum_{j=1}^{j=m} \int_{-\frac{h}{2}}^{\frac{h}{2}} \left(\int_{y_{3j}}^{y_{3j+1}} \sigma_{Fj} z_3 dy_3 \right) dz_3 ,$$

where y_{3j} and y_{3j+1} are the coordinates of the left-hand and right-hand lateral surfaces of the layer. Formula (26) is applied to determine the stress, σ_{Fj} , by replacing of ε_j with ε_{Fj} . The strain, ε_{Fj} , is obtained by replacing of κ_L with κ_F in (39). Here, κ_F is the curvature of the un-cracked beam portion.

A further one equation is written by expressing of angle of rotation of the free end of the left-hand crack arm as a function of the curvatures. For this purpose, the integrals of Maxwell-Mohr are applied [15]. The result is

$$(43) \quad \phi = \kappa_L a_1 + \kappa_Q (a_2 - a_1) + \kappa_F (l - a_2) .$$

After substituting of stresses in (41) and (42), these equations and equation (43) are solved with respect to curvatures, κ_L , κ_Q and κ_F , by using the MatLab computer program at various vales of time.

The strain energies, U_Q and U_F , are found as

$$(44) \quad U_Q = (a_2 - a_1) \sum_{j=1}^{j=m_Q} \int_{-\frac{h}{2}}^{\frac{h}{2}} \left(\int_{y_{2j}}^{y_{2j+1}} u_{0Qj} dy_2 \right) dz_2 ,$$

$$(45) \quad U_F = (l - a_2) \sum_{j=1}^{j=m} \int_{-\frac{h}{2}}^{\frac{h}{2}} \left(\int_{y_{3j}}^{y_{3j+1}} u_{0Fj} dy_3 \right) dz_3 .$$

The strain energy density, u_{0Qj} , is determined by replacing of ε_j with ε_{Qj} in formula (37). Analogically, ε_j is replaced with ε_{Fj} in (37) to obtain u_{0Fj} .

The bending moment, M , in the left-hand crack arm that is involved in (33) is found as

$$(46) \quad M = \sum_{j=1}^{j=m_L} \int_{-\frac{h}{2}}^{\frac{h}{2}} \left(\int_{y_{1j}}^{y_{1j+1}} \sigma_j z_1 dy_1 \right) dz_1 .$$

By substituting of (34), (35), (43), (44), (45) and (46), one derives

$$(47) \quad G_1 = \frac{1}{h} \left[(\kappa_L - \kappa_Q) \sum_{j=1}^{j=m_L} \int_{-\frac{h}{2}}^{\frac{h}{2}} \left(\int_{y_{1j}}^{y_{1j+1}} \sigma_j z_1 dy_1 \right) dz_1 \right. \\ \left. - \sum_{j=1}^{j=m_L} \int_{-\frac{h}{2}}^{\frac{h}{2}} \left(\int_{y_{1j}}^{y_{1j+1}} u_{0Lj} dy_1 \right) dz_1 + \sum_{j=1}^{j=m_Q} \int_{-\frac{h}{2}}^{\frac{h}{2}} \left(\int_{y_{2j}}^{y_{2j+1}} u_{0Qj} dy_2 \right) dz_2 \right].$$

Formula (47) represents the solution of the strain energy release rate for the left-hand delamination in the beam in Fig. 1. The integration in (47) is carried-out by the MatLab computer program. Formula (47) is applied to calculate the strain energy release rate at various values of time.

In order to obtain solution of the strain energy release rate for the right-hand delamination in the beam, the energy balance is written as

$$(48) \quad M\delta\phi = \frac{\partial U}{\partial a_2} \delta a_2 + G_2 h \delta a_2.$$

From (48), one derives

$$(49) \quad G_2 = \frac{1}{h} \left(M \frac{\partial \phi}{\partial a_2} - \frac{\partial U}{\partial a_2} \right).$$

By combining of (34), (35), (43), (44), (45) and (49), one obtains the following solution of the strain energy release rate for the right-hand delamination in the beam:

$$(50) \quad G_2 = \frac{1}{h} \left[(\kappa_Q - \kappa_F) \sum_{j=1}^{j=m_L} \int_{-\frac{h}{2}}^{\frac{h}{2}} \left(\int_{y_{1j}}^{y_{1j+1}} \sigma_j z_1 dy_1 \right) dz_1 \right. \\ \left. - \sum_{j=1}^{j=m_Q} \int_{-\frac{h}{2}}^{\frac{h}{2}} \left(\int_{y_{2j}}^{y_{2j+1}} u_{0Qj} dy_2 \right) dz_2 + \sum_{j=1}^{j=m} \int_{-\frac{h}{2}}^{\frac{h}{2}} \left(\int_{y_{3j}}^{y_{3j+1}} u_{0Fj} dy_3 \right) dz_3 \right].$$

The MatLab is used to perform the integration in (50). The strain energy release rate is found by (50) at various values of time.

Solutions of the strain energy release rate for the two cracks in the beam structure subjected to strains of step-like varying velocity with time are derived also by considering the complementary strain energy. For this purpose, the strain energy release rate for left-hand crack is written as:

$$(51) \quad G_1 = \frac{dU^*}{hda_1},$$

where the complementary strain energy in the beam, U^* , is found as

$$(52) \quad U^* = U_L^* + U_Q^* + U_F^*.$$

In formula (52), U_L^* , U_Q^* and U_F^* are the complementary strain energies cumulated in portions, $0 \leq x \leq a_1$ and $a_1 \leq x \leq a_2$, of the left-hand crack arm, and in the uncracked beam portion. The complementary strain energy is obtained by integrating the complementary strain energy density. Thus, formula (52) is re-written as

$$(53) \quad U^* = a_1 \sum_{j=1}^{j=m_L} \int_{-\frac{h}{2}}^{\frac{h}{2}} \left(\int_{y_{1j}}^{y_{1j+1}} u_{0Lj}^* dy_1 \right) dz_1 \\ + (a_2 - a_1) \sum_{j=1}^{j=m_Q} \int_{-\frac{h}{2}}^{\frac{h}{2}} \left(\int_{y_{2j}}^{y_{2j+1}} u_{0Qj}^* dy_2 \right) dz_2 \\ + (l - a_2) \sum_{j=1}^{j=m} \int_{-\frac{h}{2}}^{\frac{h}{2}} \left(\int_{y_{3j}}^{y_{3j+1}} u_{0Fj}^* dy_3 \right) dz_3,$$

where u_{0Lj}^* , u_{0Qj}^* and u_{0Fj}^* are the complementary strain energy densities.

The complementary strain energy density in the j -th layer of portion, $0 \leq x \leq a_1$, of the left-hand crack arm is found as

$$(54) \quad u_{0Lj}^* = \sigma_j \varepsilon_j - u_{0Lj}.$$

By substituting of (26) and (37), one derives

$$(55) \quad u_{0Lj}^* = \frac{1}{2} \theta_i \varepsilon_j^2 + \eta_{mldj} \varepsilon_j \left(\frac{\varepsilon_j - \varepsilon_{pji-1}}{t - t_{i-1}} \right)^{\frac{1}{n_j}} \\ - \frac{\eta_{mldj} n_j}{(1 + n_j) (t - t_{i-1})^{\frac{1}{n_j}}} \left[(\varepsilon_j - \varepsilon_{pji-1})^{\frac{1+n_j}{n_j}} - (-\varepsilon_{pji-1})^{\frac{1+n_j}{n_j}} \right].$$

The complementary strain energy densities, u_{0Qj}^* and u_{0Fj}^* , are obtained by replacing of ε_j with ε_{Qj} and ε_{Fj} in formula (55), respectively.

By substituting of (53) in (51), one obtains

$$(56) \quad G_1 = \frac{1}{h} \left[\sum_{j=1}^{j=m_L} \int_{-\frac{h}{2}}^{\frac{h}{2}} \left(\int_{y_{1j}}^{y_{1j+1}} u_{0Lj}^* dy_1 \right) dz_1 - \sum_{j=1}^{j=m_Q} \int_{-\frac{h}{2}}^{\frac{h}{2}} \left(\int_{y_{2j}}^{y_{2j+1}} u_{0Qj}^* dy_2 \right) dz_2 \right].$$

The MatLab computer program performs the integration in (56). The strain energy release rate is calculated by using (56) at various values of time.

The strain energy release rate for the right-hand crack is expressed as

$$(57) \quad G_2 = \frac{dU^*}{hda_2}.$$

By combining of (53) and (57), one derives

$$(58) \quad G_2 = \frac{1}{h} \left[\sum_{j=1}^{j=m_Q} \int_{-\frac{h}{2}}^{\frac{h}{2}} \left(\int_{y_{2j}}^{y_{2j+1}} u_{0Qj}^* dy_2 \right) dz_2 - \sum_{j=1}^{j=m} \int_{-\frac{h}{2}}^{\frac{h}{2}} \left(\int_{y_{3j}}^{y_{3j+1}} u_{0Fj}^* dy_3 \right) dz_3 \right].$$

Formula (58) is used to calculate the strain energy release rate at various values of time. The integration is carried-out by the MatLab computer program.

The strain energy release rates obtained by using solutions (56) and (58) are exact matches of these found by using (47) and (50). This fact is a verification of the analysis developed in the present paper.

3 PARAMETRIC INVESTIGATION

The parametric investigation performed in this section of the paper aims to evaluate the influence of various parameters on the strain energy release rate for the two delamination cracks in the multilayered non-linear viscoelastic beam subjected to strains whose velocity varies step-like with time. It is assumed that $b = 0.015$ m, $h = 0.020$ m, $l = 0.400$ m, $m_L = 3$, $m_Q = 5$, $m = 7$, $s = 3$, $n_j = 1.5$, $v_{\phi_1} = 0.2 \times 10^{-7}$ s⁻¹, $v_{\phi_2} = 0.5 \times 10^{-7}$ s⁻¹ and $v_{\phi_3} = 0.7 \times 10^{-7}$ s⁻¹.

First, the variation of the strain energy release rate with time is investigated. With solutions given in Section 2 of the present paper, it is straightforward to calculate the strain energy release rate at various values of time. The left-hand delamination crack is considered. The strain energy release rate is expressed in non-dimensional form by applying the formula $G_N = G/(E_{01}h)$. In Fig. 5, the non-dimensional strain energy release rate versus non-dimensional time curve is plotted. The time is presented in non-dimensional form by using the formula $t_N = tE_{01}/\eta_{01}$. From Fig. 5, it is obvious that the strain energy release rate increases with time. Figure 5 indicates also that at $t = t_1$ and $t = t_2$, the slope of the strain energy release rate-time curve increases (this is due to step-like increase of the velocity of strains at $t = t_1$ and $t = t_2$).

The variation of the strain energy release rate with the parameter, λ_1 , is investigated for both delamination cracks in the beam (Fig. 1). The non-dimensional strain energy release rate versus λ_1 curve is plotted in Fig. 6. It is clear from Fig. 6 that

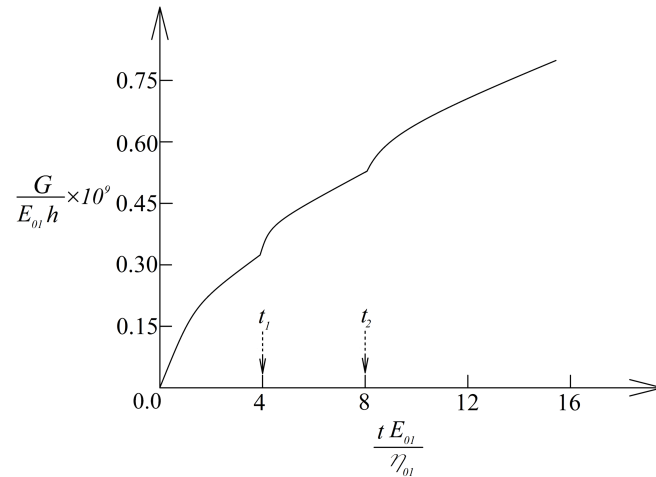


Fig. 5: The non-dimensional strain energy release rate plotted versus non-dimensional time.

increase of λ_1 reduces the strain energy release rate. The curves in Fig. 6 show that the strain energy release rate for the left-hand delamination crack is higher in comparison with that for the right-hand delamination crack. The behaviour is explained by the fact that the stiffness of the left-hand crack arm in portion, $a_1 \leq x \leq a_2$, is higher than that in portion, $0 \leq x \leq a_1$.

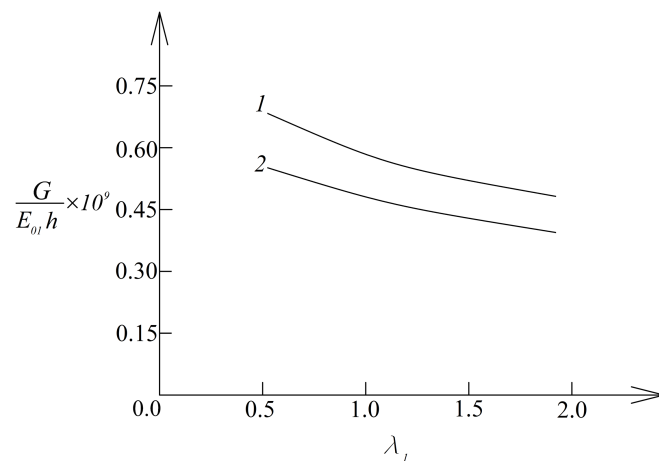


Fig. 6: The non-dimensional strain energy release rate plotted versus λ_1 (curve 1 – for the left-hand delamination, curve 2 – for the right-hand delamination).

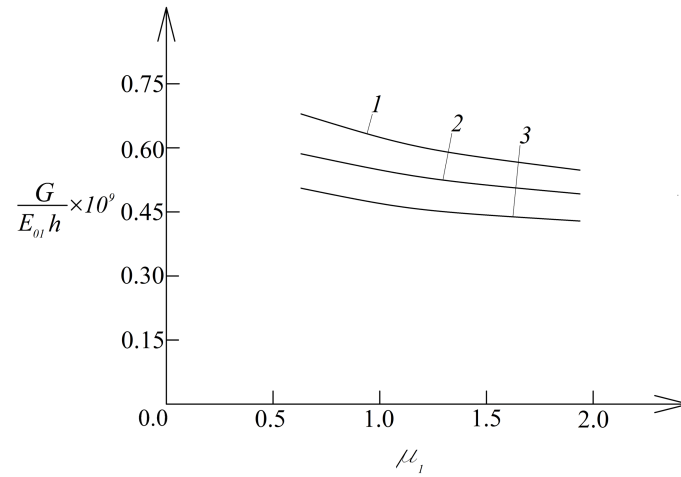


Fig. 7: The non-dimensional strain energy release rate plotted versus μ_1 (curve 1 – at $E_{02}/E_{01} = 0.5$, curve 2 – at $E_{02}/E_{01} = 1.5$ and curve 3 – at $E_{02}/E_{01} = 2.5$).

The influence of the variation of η_1 along the width layer 1 on the strain energy release rate is studied by carrying-out calculations of the strain energy release rate at various values of μ_1 . In Fig. 7, the non-dimensional strain energy release rate versus μ_1 curve is plotted at three E_{02}/E_{01} ratios for the left-hand delamination crack. It

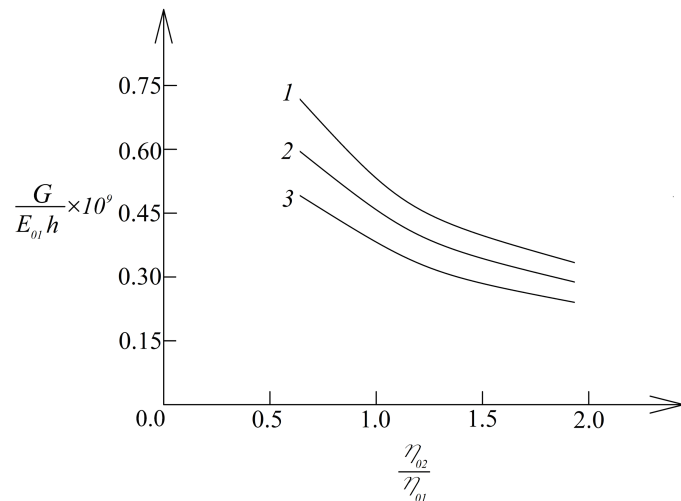


Fig. 8: The non-dimensional strain energy release rate plotted versus η_{02}/η_{01} ratio (curve 1 – at $\omega_1 = 0.5$, curve 2 – at $\omega_1 = 2.0$ and curve 3 – at $\omega_1 = 3.0$).

can be observed in Fig. 7 that the strain energy release rate decreases with increasing of μ_1 . The increase of E_{02}/E_{01} ratio reduces the strain energy release rate (Fig. 7).

Finally, the effects of η_{02}/η_{01} ratio and the variation of η_{0ndl1} along the width of layer 1 on the strain energy release rate are analysed. The results obtained are displayed in Fig. 8 where the non-dimensional strain energy release rate versus η_{02}/η_{01} ratio curve is plotted at three values of ω_1 for the left-hand delamination crack. The parameter, ω_1 , characterizes the variation of η_{0ndl1} along the width of layer 1. From curves shown in Fig. 8, we found that increase of η_{02}/η_{01} ratio reduces the strain energy release rate. The increase of parameter, ω_1 , leads also to reduction of the strain energy release rate (Fig.8).

4 CONCLUSIONS

The delamination of a non-linear viscoelastic multilayered beam structure subjected to strains of step-like varying velocity with time is analysed. A viscoelastic model with a linear spring, a linear dashpot and a non-linear dashpot is used for describing the mechanical behaviour of the beam. The non-linear constitutive law of the model under strains whose velocity varies step-like with time is obtained. For this purpose, the differential equation of the model is worked-out and solved. Since the layers of the beam exhibit material inhomogeneity along the width, the material properties of the viscoelastic model are function of the coordinate in the width direction of the beam. Two delamination cracks are located arbitrary along the width of the beam. The left-hand crack arm is loaded in bending so as the velocity of the angle of rotation this crack arm varies step-like with time. Solutions of the strain energy release rate are derived for both delamination cracks by analysing the balance of the energy. The solutions take into account the non-linear viscoelastic behaviour of the beam under strains of step-like varying velocity. The strain energy release rate is found also be considering the complementary strain energy for verification. A parametric investigation of the strain energy release rate is performed for both delamination cracks. It is found that the slope of strain energy release rate – time curves increases at the moment of time in which the velocity of the strain increases step-like. The study reveals that the strain energy release rate for the left-hand delamination crack is higher in comparison with that for the right-hand delamination crack. The analysis shows that increasing of parameters, λ_1 , μ_1 and ω_1 , reduces the strain energy release rate decreases. The increases of E_{02}/E_{01} and η_{02}/η_{01} ratios lead to reduction of the strain energy release rate. The analysis developed in the present paper reveals the characteristics of delamination of non-linear viscoelastic multilayered beams under strains of step-like varying velocity.

ACKNOWLEDGMENTS

V. Rizov gratefully acknowledges the financial support by the German Academic Exchange Organization (DAAD) for his research stay in Department of Engineering Mechanics, Institute of Mechanics, Otto-von-Guericke-University, Magdeburg, Germany.

REFERENCES

- [1] A. NEUBRAND, J. RÖDEL (1997) Gradient materials: An overview of a novel concept. *Zeitschrift für Metallkunde* **88** 358-371.
- [2] M. GASIK (2010) Functionally graded materials: bulk processing techniques. *International Journal of Materials and Product Technology* **39** 20-29.
- [3] M. NEMAT-ALLAL, M. ATA, M. BAYOUMI, W. KHAIR-ELDEEN (2011) Powder metallurgical fabrication and microstructural investigations of Aluminum/Steel functionally graded material. *Materials Sciences and Applications* **2** 1708-1718.
- [4] Y. ZHANG, M. SUN, D. ZHANG (2012) Designing functionally graded materials with superior load-bearing properties. *Acta Biomaterialia* **8** 1101-1108.
- [5] G. UDUPA, S. SHRIKANTHA RAO, K. RAO GANGADHARAN (2014) Functionally Graded Composite Materials: An Overview. *Procedia Materials Science* **5** 1291-1299.
- [6] S. BOHIDAR, R. SHARMA, P. MISHRA (2014) Functionally graded materials: A critical review. *International Journal of Research* **1** 289-301.
- [7] M. EL-WAZERY, A. EL-DESOUKY (2015) A review on functionally graded ceramic-metal materials. *Material Environment Science* **6** 1369-1376.
- [8] M. NAEBE, K. SHIRVANIMOGHADDAM (2016) Functionally graded materials: A review of fabrication and properties. *Applied materials today* **5** 223-245.
- [9] R. MAHAMOOD, E. AKINLABI (2017) "Functionally Graded Materials". Springer.
- [10] I. MARKOV, D. DINEV (2005) Theoretical and experimental investigation of a beam strengthened by bonded composite strip. In: *Reports of International Scientific Conference VSU'2005*.
- [11] J.S. KIM, K.W. PAIK, S.H. OH (1999) The Multilayer-Modified Stoney's Formula for Laminated Polymer Composites on a Silicon Substrate. *Journal of Applied Physics* **86** 5474-5479.
- [12] M. FINOT, S. SURESH (1996) Small and large deformation of thick and thin-film multilayers: effect of layer geometry and compositional gradients. *Journal of the Mechanics and Physics of Solids* **44** 683-721.
- [13] V. RIZOV (2020) Analysis of Two Lengthwise Cracks in a Viscoelastic Inhomogeneous Beam Structure. *Engineering Transactions* **68** 397-415.
- [14] V. RIZOV (2021) Delamination crack study of a multilayered inhomogeneous beam exhibiting stress relaxation. *Journal of Theoretical and Applied Mechanics* **51** 407-420.
- [15] V. Zubchaninov (1990) "Fundamentals of Theory of Elasticity and Plasticity". Vishaya Shkola.